# Design of Heat Insulation Mechanism for Ultra-low Temperature Liquid Level Detection

Senlin Cheng[1,a], Xinyi Xia[*1,b1], and Xin Shi[1,c]
[1*]School of Automation, Chongqing Univ., Chongqing, PR China.

## ABSTRACT.

In order to solve the problem that the liquid level measuring mechanism of ultra-low temperature liquid such as LNG is too complicated, a design method of sensor heat insulation mechanism is proposed, so that the instrument can complete the non-contact detection of ultra-low temperature liquid under normal temperature environment. The thermal insulation mechanism is determined according to the measurement process, the heat transfer model of the measurement channel is established, the control structure of the thermal insulation channel is determined, and the functional relationship between its size and heat transfer is established. Finally, the dimensional correlation relationship under the minimum heat transfer is obtained by extreme value optimization. In the typical ultra-low temperature liquid level measurement conditions, the actual structure size and temperature control effect were calculated and verified. Through the comparison with the finite element simulation structure of the structure, it was proved that the proposed thermal insulation mechanism can meet the temperature isolation and heat dissipation control requirements of the ultra-low temperature liquid level.

**Keywords:** Ultra-low temperature liquid; Non-contact liquid level detection; Finite element analysis.

## 1. INTRODUCTION

Liquefied natural gas (LNG), as a clean, efficient and high-quality energy, is playing an increasingly important role in optimizing the national energy consumption structure, controlling greenhouse gas emissions, and improving the atmospheric environment.LNG is generally stored in a container with a temperature of 93K and a pressure of 0.1MPa, with a volume ratio of about 1:625 and a volumetric energy density of about 72% of gasoline. In 2020, global LNG trade achieved incremental growth for the sixth consecutive year, setting a new record for the past decade [1]. However, under the condition of high liquid level storage, the ultra-low temperature storage tank is prone to abnormal increase of evaporated gas (BOG), resulting in tumbling, overpressure and other accidents. Liquid level detection can predict tank reserves, improve early warning measures under high liquid level conditions, and ensure operation safety.

In 2022, Qiang Chen et al. [2] studied a fiber optic sensor that combined SI and MMI for level and strain measurement. SMF-NCF-SMF structure was used to excite multi-mode interference (MMI), and the level sensitivity reached 525pm/mm. The Panda polarization-preserving fiber (PMF) is used to generate polarization mode interference in the Sagnac ring with a strain sensitivity of 33 pm/με. In 2020, Jayalaxmi [3] proposed a design that changed the electrode structure from the traditional design to the spiral structure. Under standard test conditions, the sensitivity of the spiral CLS structure increased by 99.99%, with higher sensitivity and lower sensor delay compared with the parallel rod and cylindrical CLS. In 2018, Yingzi Zhang et al. [4] proposed a continuous liquid level sensor based on the spiral structure of double parallel plastic fiber (POF). By measuring the side coupling power in the passive fiber, the sensitivity of 0.0208μW/mm can be obtained for a small curvature radius of 5mm, and the measurement range can also be extended to 120mm. In 2019, Chen zhu [5] reported a non-contact liquid sensor based on microwave Fabry-Perot resonator, which used the inner and outer conductors of hollow coaxial cable. In the experiment, the water-oil interface and oil-ethanol interface were measured, and the sensor resolution was about 23μm. In 2018, Li Yijian et al. [6] of Zhejiang University adopted a double-layer coaxial capacitor structure for the measurement of low temperature liquid level and realized liquid level measurement through calibration experiment. The average sensitivity of the liquid level gauge was 46.76pF/m, and the relative error of liquid level measurement was within 0.23%. The structure of contact measurement is complicated, the generality is poor, the cost is high, and the heat loss is easy to cause BOG anomaly. Considering that the measurement object in this paper is ultra-low

[1a]csl@cqu.edu.cn, [b*]915634402@qq.com, [c]1419209780@qq.com

The International Conference Optoelectronic Information and Optical Engineering (OIOE2024), edited by Yang Yue, Lu Leng, Proc. of SPIE Vol. 13513, 135130X · © 2025 SPIE · 0277-786X · © The Authors.
 · doi: 10.1117/12.3045424

temperature liquid in liquid storage tank, the measurement range of detection sensors is high, so direct contact liquid level measurement, such as float, capacitance and other sensors are not applicable, while optical, ultrasonic, radar and other sensors are suitable for a wide range of measurement requirements [7], and non-contact measurement liquid level meter has the advantages of high precision, simple structure and high reliability. However, it is still necessary to solve the adaptability problem of ultra-low temperature liquid temperature environment.

This paper presents a insulation layer structure and measurement channel for liquid level detection. Through the optimized combination of size, the non-contact liquid level meter can realize the high-precision liquid level detection at normal temperature while ensuring the minimum heat loss. The validity and rationality of the detection scheme were verified by Ansys finite element analysis and simulation.

## 2. ADIABATIC DESIGN

### 2.1 Analysis of Heat Transfer Process of Measuring Mechanism

The composition of the detection mechanism is shown in Figure 1: the liquid storage tank is equipped with the tested ultra-low temperature liquid, and its liquid level is reflected by the float in the pipeline with the liquid level. A heat resistance channel is installed at the pipe entrance of the liquid storage tank to ensure that the measuring instrument works in the normal temperature environment under the ultra-low temperature liquid environment in the tank. The reflective ranging sensor transmits pulses and receives echoes from the measuring hole in the thermal resistance channel to realize non-contact measurement. A transparent cover plate is arranged between the sensor and the heat resistance channel to ensure the passage of the sensor measurement wave and realize the isolation of the high pressure in the measurement environment and the normal pressure in the sensor box. A fan is placed in the instrument cover to circulate the heat inside the instrument cover and ensure the consistent temperature of the sensor layer.

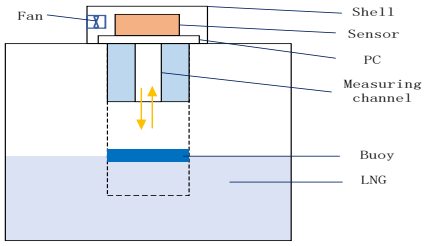


Figure. 1 Schematic Diagram of Testing Mechanism

When the sensor is working, there is heat transfer between the external environment and the internal ultra-low temperature liquid. The form of internal and external heat transfer is mainly heat conduction, and the direction of heat transfer is from the object with high temperature to the object with low temperature. Since the indoor ambient temperature is higher than the temperature of the ultra-low temperature liquid in the tank, the heat is transmitted from the environment through the instrument cover and the insulation layer to the tank, simplifying its heat transfer path as shown in Figure 2. Indoor ambient temperature is $t_{w1}$; The temperature of the cooling fan inside the instrument cover is $t_{w2}$ because it is the same. The temperature at the upper end of the heat resistance aisle is$t_{w3}$. The ultra-low temperature liquid temperature is $t_{w4}$. The thermal conductivity resistance of the instrument cover is $R_{\lambda 1}$, the thermal conductivity resistance of the transparent cover is $R_{\lambda 2}$, and the thermal conductivity resistance of the thermal insulation layer and the thermal insulation hole is $R_{\lambda 3}$ and $R_{\lambda 4}$, respectively.

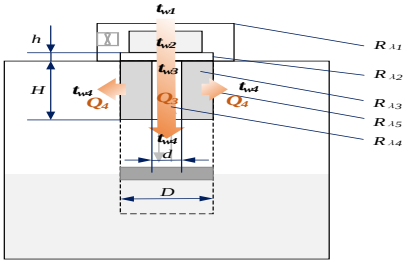


Figure. 2 Heat Influence Diagram of the Measurement Process

In order to prevent the entry of external heat leading to the evaporation of ultra-low temperature liquid, the heat transfer channel should be optimized to reduce the heat transfer efficiency, and the temperature difference between the inside and outside of the sensor housing should be controlled to ensure that the temperature of the sensor room is within the operating range of the normal temperature instrument.

### 2.2 Thermal Insulation Mechanism Parameter Design

The heat transfer process in Figure 2 can be simplified as Figure 3, $R_{\lambda 3}, R_{\lambda 4}$ and $R_{\lambda 5}$ are in parallel and form a total thermal resistance in series with $R_{\lambda 1}$ and $R_{\lambda 2}$. According to the principle of one-way heat transfer, due to the temperature difference between the upper and lower levels, the heat inside the system will be transferred from the higher level to the lower level, and the heat transfer of the entire insulation layer mechanism can be calculated using the one-way heat transfer formula [8], thus obtaining the heat transfer power as follows:

$$Q = \frac{t_{w1} - t_{w4}}{R_{\lambda 1} + R_{\lambda 2} + \frac{R_{\lambda 3} \cdot R_{\lambda 4} \cdot R_{\lambda 5}}{R_{\lambda 3} \cdot R_{\lambda 5} + R_{\lambda 4} \cdot R_{\lambda 5} + R_{\lambda 3} \cdot R_{\lambda 4}}} \tag{1}$$

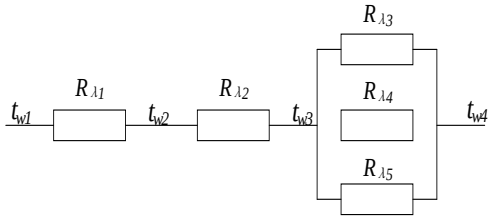


Figure. 3 Equivalent Heat Transfer Path

If the area of the instrument cover is S, the wall thickness is $\delta$, and the thermal conductivity is $\lambda_1$.Set the thermal conductivity of the thermal resistance material as $\lambda_3$, the thermal conductivity of the gas after ultra-low temperature liquid gasification as $\lambda_4$, and the thermal conductivity of the transparent PC plate as $\lambda_2$, h is the thickness of the PC board,where D is the overall diameter of the insulation layer, d is the diameter of the measured aperture, and H is the height and size parameter of the insulation layer , and the thermal resistance of each part can be obtained:

$$\begin{cases} R_{\lambda 1} = \dfrac{\delta}{\lambda_1 S} \\ R_{\lambda 2} = \dfrac{4h}{\pi D^2 \lambda_2} \\ R_{\lambda 3} = \dfrac{4H}{\pi \lambda_3 (D^2 - d^2)} \\ R_{\lambda 4} = \dfrac{4H}{\pi d^2 \lambda_4} \\ R_{\lambda 5} = \dfrac{\ln\left(\frac{D}{d}\right)}{\pi \cdot \lambda_3 \cdot H} \end{cases} \tag{2}$$

$R_{\lambda 1}$ is related to the outer cover material, wall thickness and area of the sensor, in order to ensure that the temperature difference between the inside and outside the sensor cover is small enough, the outer cover with thin wall, good heat transfer performance and large area is generally selected, compared with $R_{\lambda 2}$, $R_{\lambda 3}$, $R_{\lambda 4}$, $R_{\lambda 5}$,when estimating heat transfer power $R_{\lambda 1}$ can be ignored. In general, the thermal conductivity of transparent glass is $\lambda_2$, much higher than that of gas after ultra-low temperature liquid gasification is $\lambda_4$, and h<H. When estimating heat transfer power, compared with $R_{\lambda 3}$, $R_{\lambda 4}$, $R_{\lambda 5}$, the thermal resistance $R_{\lambda 2}$ is smaller.

When considering the heat transfer process of the insulation layer structure, the overall heat transfer process can be simplified into two one-dimensional heat transfer processes, namely, two one-dimensional steady heat transfer processes of $Q_3$ along the height z direction and $Q_4$ along the radius r direction.

In the direction of $Q_3$, the measurement channel of the cylinder and the thermal resistance material are uniform and isotropic along the height direction respectively, and the temperature changes linearly. It can be assumed that the heat transfer also changes linearly along the height direction. The thermal resistance of the two is in parallel, that is, the heat transfer $Q_3$ is:

$$Q_3 = \frac{t_{w1} - t_{w4}}{\frac{R_{\lambda 3} \cdot R_{\lambda 4}}{R_{\lambda 3} + R_{\lambda 4}}} = \frac{t_{w3} - t_{w4}}{\frac{4H}{\pi D^2 \lambda_3 + \pi d^2 (\lambda_4 - \lambda_3)}} \tag{3}$$

In the $Q_4$ direction, the material of the cylinder is uniform and isotropic along the radius direction, and the temperature changes linearly. It can be assumed that the heat dissipation also changes linearly along the radius direction. Then the heat transfer from the radius direction is a single-layer cylindrical wall, and its heat transfer is $Q_4$:

$$Q_4 = \frac{2\pi\lambda_3 H(t_m - t_{w4})}{\ln\left(\frac{D}{d}\right)} \tag{4}$$

$$Q = Q_3 + Q_4 = \frac{1}{4H}[\pi D^2 \lambda_3 + \pi d^2 (\lambda_4 - \lambda_3)](t_{w3} - t_{w4}) + \frac{2\pi\lambda_3 H(t_m - t_{w4})}{\ln\left(\frac{D}{d}\right)} \tag{5}$$

The temperature $t_m$ on the inner wall of the cylinder is approximately a constant value, that is $t_m = \frac{t_{w3}+t_{w4}}{2}$. According to the calculation formula (5) of the total heat transfer Q, when the minimum value of Q is taken to ensure the minimum heat transfer through the insulation layer, there are:

$$H = \sqrt{\frac{[\pi D^2 \lambda_3 + \pi d^2 (\lambda_4 - \lambda_3)](t_{w3} - t_{w4}) \cdot \ln\left(\frac{D}{d}\right)}{8\pi\lambda_3 (t_m - t_{w4})}} \tag{6}$$

If $D = nd$ is defined, where n is the structural coefficient, then the height dimension H of the insulation layer at the minimum value of the total heat transfer Q can be expressed as:

$$H = \sqrt{\frac{(t_{w3} - t_{w4}) \cdot \pi \cdot d^2 \cdot (\lambda_3 \cdot (n^2 - 1) + \lambda_4) \cdot \ln(n)}{8\pi\lambda_3 (t_m - t_{w4})}} \tag{7}$$

**2.3 Structural Size Calculation under Typical Measurement Conditions**

According to the measurement process requirements, determine $d = 20mm$. Select the ultra-low temperature liquid as liquefied natural gas, the storage temperature is $t_{w4} = -180℃$， , and $t_{w3} = 0℃$, the thermal conductivity of LNG gas is $\lambda_4 = 0.03W/(m \cdot K)$, the thermal insulation layer is selected as polyurethane insulation material, thermal conductivity $\lambda_3 = 0.024W/(m \cdot K)$

According to formula (7), the relationship between the height of the insulation layer H and the structural coefficient n under the lowest heat transfer can be obtained, as shown in Figure 4. It can be seen that based on the principle of minimum value of the total heat transfer Q of the insulation layer, the height H of the insulation layer also increases with the increase of the proportional coefficient n, and the two are in a direct proportional relationship.

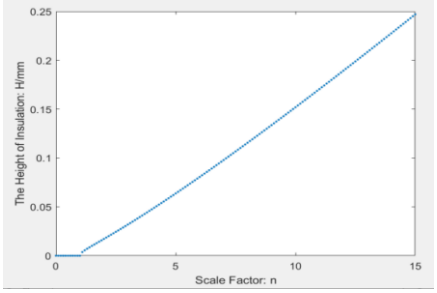


Figure. 4 H function curve of insulation layer height

When the proportional coefficient $n = 5$, in the case of the minimum total heat transfer, the height of the insulation layer $H_0 = 0.0637\text{m}$, the total heat transfer $Q = 1.0751\text{W}$. If some free changes are made to $H$, the relationship between $H$ and heat transfer $Q$ can be obtained as shown in Figure 5, and the height of insulation layer $H_0$ is near the minimum value of $Q$.

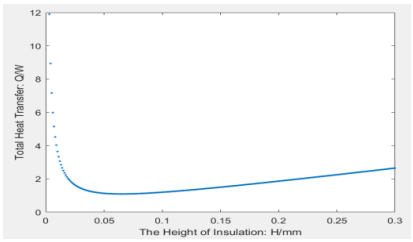


Figure. 5 Total Heat Transfer Q Function Curve

### 2.4 Measurement Channel Temperature Distribution Calculation

Indoor ambient temperature is $t_{w1} = 20℃$, LNG temperature environment is $t_{w4} = -180℃$, the instrument cover shell is made of stainless steel, its thermal conductivity $\lambda_1 = 14.986\text{W}/(\text{m}\cdot\text{k})$, subject to process restrictions, the thickness of stainless steel plate is generally $2\text{mm}$. The thermal conductivity of polycarbonate (PC) $\lambda_2 = 0.19\text{W}/(\text{m}\cdot\text{k})$, the radius size of transparent PC board $r_1 = D/2$, the height $\delta = 0.03\text{m}$. Calculate the thermal resistance of each part, $R_{\lambda 1} = 0.017, R_{\lambda 2} = 20.104, R_{\lambda 3} = 353.678, R_{\lambda 4} = 6790.611, R_{\lambda 5} = 333.529$, substituting into equation (1), it can be obtained that the heat flux through the entire adiabatic mechanism $Q_0 = 1.066\text{W}$. By calculating the temperature distribution of the entire adiabatic mechanism based on the serial-parallel relationship of each thermal resistance in Figure 3, the working temperature $t_{w2}$ of the sensor layer and the temperature $t_{w3}$ at the top of the insulation layer can be obtained:

$$t_{w2} = t_{w1} - Q_0 \cdot R_{\lambda 1} = 19.982℃ \tag{8}$$

$$t_{w3} = t_{w2} - Q_0 \cdot R_{\lambda 2} = 1.457℃ \tag{9}$$

The calculated $t_{w3}$ is basically consistent with the assumed $t_{w3}$ in Section 2.3 under the condition that the structure coefficient n=5, and the heat flux Q of the whole structure is basically consistent with the theoretical minimum value in Section 2.3. At this time, $t_{w2} = 19.982℃$, so the sensor can be realized to work in normal temperature environment.

## 3. FINITE ELEMENT ANALYSIS OF ADIABATIC STRUCTURES

### 3.1 Simulation Analysis

In the second section, the heat transfer process of the whole structure is simplified and analyzed, and the size parameters of the insulation layer structure are designed based on the principle of minimum heat flux. Now the simulation model and simulation environment are built under Ansys 2020R2 software to verify the correctness of the theoretical calculation in section 2.3 and the consistency of the curve change trend. The bottom end of the insulation layer structure and the side end along the radius direction are in the temperature environment of $t_{w4} = -180℃$, only the top part of the insulation layer structure is in the temperature environment of $t_{w3} = 0℃$, then its boundary conditions can be set. Since the research content of this paper is mainly aimed at the steady-state thermodynamic properties of the insulation structure, other material

parameters of each component, such as Poisson's ratio, elastic modulus and density, are set by software default, mainly for the thermodynamic parameters of the material.The structure and temperature parameters of each part of the overall structure are shown in Table 1.

Table 1. Physical Performance Parameters of Each Part

| Physical property | Argument |
|---|---|
| Temperature of the upper end of the heat resistance aisle $t_{w3}$ | 0℃ |
| Ultra-low temperature liquid ambient temperature $t_{w4}$ | −180℃ |
| Measurement channel aperture size d | 20mm |
| Outer diameter of insulation layer D | 100mm |
| The thermal conductivity of natural gas $\lambda_3$ | $0.03\ W \cdot m^{-1} \cdot K^{-1}$ |
| Thermal conductivity of polyurethane $\lambda_4$ | $0.024\ W \cdot m^{-1} \cdot K^{-1}$ |

### 3.2 Simulation Modeling

#### 3.2.1 Model Assumption

Due to the complexity of the design detection structure, the following initial conditions and assumptions are set for it to facilitate the simulation calculation [9] :

The research object is LNG transported and stored in the liquid storage tank. The temperature field distribution of the detection structure and the trend of the overall heat flux changing with the height of the insulation layer are analyzed and verified. In the whole structure, the heat conduction through the sunken shell, the various supports and holes of the measuring cover plate are ignored, and the insulation layer is considered to be evenly distributed.

Set the LNG temperature in the tank to $-180\,°C$ and the ambient temperature to $0\,°C$.

The idea that all materials are isotropic and uniform.

#### 3.2.2 Meshing

The original structure contains bolts, washers and other auxiliary structures. As these auxiliary structures have negligible influence on the heat insulation performance of the original structure, the structure of these auxiliary parts is complex and there are many small surfaces, and the model grid division is required in the modeling process, so the convergence and efficiency of calculation are greatly affected [10]. In order to reduce the amount of computation, similar auxiliary components were deleted in this simulation, and the design of thermal insulation structure was reasonably simplified. In order to reduce the amount of computation, the mesh cell size was defined as 10mm, and the grid division tool was used to divide the model into hexahedral networks. The schematic schematic diagram of the simplified structure of the insulation layer is shown in Figure 6 below.

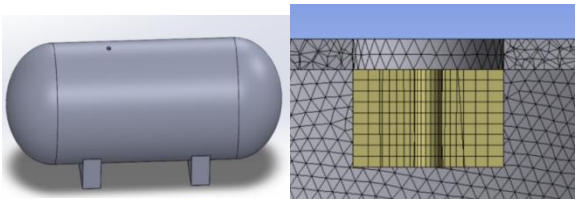

Figure. 6 Schematic Diagram of Insulation Structure

### 3.3 Simulation Result Analysis

Figure 7 is the schematic diagram of the temperature field distribution of the overall structure. It can be seen that the temperature distribution gradually decreases from the top to the side end and the bottom end, and the change trend is circular. The structure was simulated, and the height size H of the insulation layer was changed from $5-300mm$ to record the corresponding heat flux Q, and the line between the heat flux Q and height size H was drawn by Excel, and

compared with Figure 5, as shown in Figure 8, it can be seen that the trend of change was basically the same, and both showed concave curves with openings upward, and the curves basically coincided. It can be verified that the insulation layer height dimension parameter H designed by the principle of minimum heat flux Q is reasonable and effective.

## 4. CONCLUSION

This paper proposes a detection scheme for ultra-low temperature liquid measurement under normal temperature environment based on conventional instruments. The insulation layer is designed, and the 3D finite element model built is analyzed and simulated to draw the following conclusions:

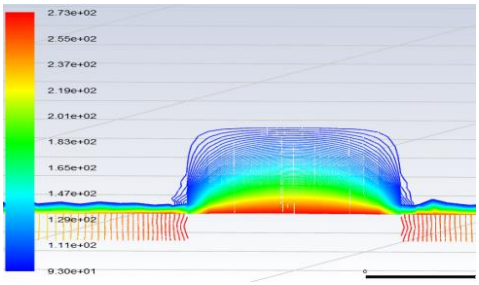


Figure. 7 Temperature field distribution diagram of the whole structure

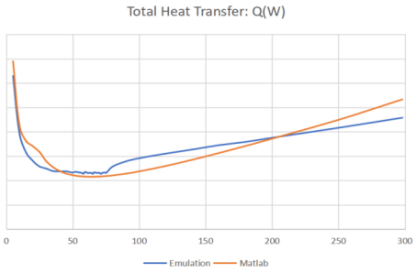


Figure. 8 Heat Flux Q Function Curve

The height dimension parameter H of the insulation layer structure is designed according to the principle of minimum value of heat flux Q. It can be obtained that the height H of the insulation layer increases with the increase of the proportional relationship n between the overall diameter D of the insulation layer and the diameter d of the measurement channel, and the relationship is proportional.

The influence of the change of the height and size of the insulation layer on the heat flux of the insulation layer is non-linear, and the change trend shows a concave curve with the opening upward, and there is a minimum heat flux. Through the analysis of the curve, it can be seen that the trend change of the function on the left of the extreme value point is more sensitive, and the change of the function on the right is smoother.

Through the theoretical calculation of the heat transfer process of the whole detection structure, it is verified that the sensor can realize the non-contact measurement of ultra-low temperature liquid at normal temperature, that is $t_{w2} = 19.982℃$, while ensuring the minimum heat loss.

The simulation environment is built in Ansys, and the model heat transfer simulation is carried out. By comparing the theoretical and simulated heat flux curves, it can be seen that the curve changes in the same trend, and it is verified that the design of the height size H of the insulation layer based on the principle of the minimum heat flux Q can achieve the minimum heat flux Q under the current proportional coefficient. This scheme is feasible, so the structural design of this paper is of guiding significance for practical work.

## 5. ACKNOWLEDGMENTS

This work is supported by Development and Application of Intelligent Composite Sensor System for LNG Cryogenic Liquefied Natural Gas(cstc2021jscx-gksbX0047).

## 6. REFERENCE


[1] Chao Y ,Yan L ,Fei P . Comparative study of three insulation materials installed on type C independent tank for offshore LNG transportation[J]. Cryogenics,2022,126.

[2] Qiang C ,Hailiang C ,Yundong L , et al. An optical fiber sensor for the detections of liquid level and strain through cascading Sagnac interference and modal interference[J]. Infrared Physics and Technology,2022,127.

[3] Hanni R J ,Venkata K S . A novel helical electrode type capacitance level sensor for liquid level measurement[J]. Sensors and Actuators: A. Physical,2020,315.

[4] Zhang Y,Hou Y,Zhang Y. Continuous liquid level detection based on two parallel plastic optical fibers in a helical structure[J]. Optical Engineering,2018,57(2).

[5] Zhu C ,Zhuang Y ,Chen Y , et al. Contactless Liquid Interface Measurement based on a Hollow Coaxial Cable Resonator[J]. Sensors & Actuators: A. Physical,2018,285.

[6] Li Yijian, Wu Shuqin, Jin Tao. Optimization and experiment of low temperature slurry capacitive liquid level meter [ J ].Journal of Zhejiang University ( Engineering Edition ), 2018,52 ( 05 ) : 966-970 + 1019.

[7] Hanni R J ,Venkata K S . Does the existing liquid level measurement system cater the requirement of future generation?[J]. Measurement,2020,156.

[8] Linna Z. Analysis of energy saving effect of green building exterior wall structure based on ANSYS simulation analysis[J]. Environmental Technology & Innovation,2021,23.

[9] Xiaofeng X,Xuelai Z. Simulation and experimental investigation of a multi-temperature insulation box with phase change materials for cold storage[J]. Journal of Food Engineering,2021,292.

[10] Zhou, J, Su, J. Y. (2017). ANSYS Workbench Finite Element Analysis and Detailed Examples [M]. Beijing: People's Posts and Telecommunications Press.